

Warm multi-natural inflation

Asuka Ito ^{a,1} and Rudnei O. Ramos ^b

^aDepartment of Physics, Kobe University, Kobe 657-8501, Japan

^bDepartamento de Física Teórica, Universidade do Estado do Rio de Janeiro, 20550-013 Rio de Janeiro, RJ, Brazil

E-mail: asuka@phys.sci.kobe-u.ac.jp, rudnei@uerj.br

Abstract.

Multi-natural inflation is studied in the context of warm inflation. We study the warm multi-natural inflation scenario with both linear and cubic temperature-dependent dissipation coefficients. The model is motivated by axion-like inflation models with coupling to non-Abelian gauge fields through a dimension-five coupling and dissipation originating from sphaleron decay in a thermal bath. Both cases of dissipation coefficients can be compatible with current observations. In the case of the cubic dissipation coefficient, we find that the curvature perturbation starts to grow suddenly when a transition from a weak dissipation to a strong dissipation regime occurs at the later stage of the inflation. We also show that such rapid growth of the curvature perturbation on small scales gives rise to abundant scalar induced gravitational waves, which may be detectable with future gravitational wave detectors such as DECIGO and ET. On the other hand, there are also other parameter regions of the model, in the warm inflation regime of weak to strong dissipation and with sub-Planckian axion decay constant, that can lead to overproduction of primordial black holes on small scales, which are constrained by nucleosynthesis bounds, thus ruling out the model in this region of parameters.

ArXiv ePrint: [2504.15606](https://arxiv.org/abs/2504.15606)

¹Corresponding author.

Contents

1	Introduction	1
2	warm multi-natural inflation	2
3	Background dynamics and perturbation quantities in WI	4
4	Numerical Results	7
4.1	Linear dissipation coefficient	8
4.2	Cubic dissipation coefficient	8
4.3	Discussion of the results	10
5	Induced gravitational waves	12
6	Conclusion	13
A	Spectral tilt in the multi-natural WI model	15

Contents

1 Introduction

Inflationary cosmology has profoundly shaped our understanding of the early universe, providing robust solutions to the horizon and flatness problems while seeding primordial density fluctuations. Inflation models can be classified into two main categories: *cold inflation* (CI) and *warm inflation* (WI) models. In the traditional CI model, a supercooled universe is followed by a post-inflationary reheating phase to generate the hot Big Bang. On the other hand, WI [1] proposes a scenario in which the inflaton field continuously dissipates energy into a thermal radiation bath during inflation, rather than after. This paradigm avoids supercooling, naturally sustains slow-roll through dissipative dynamics, and seamlessly transitions to a radiation-dominated era without a distinct reheating phase [2–4]. Moreover, warm inflation’s thermal fluctuations offer distinct observational signatures, such as modified primordial power spectra and non-Gaussianities, testable against cosmic microwave background (CMB) data [5–9] (for recent work confronting different WI models with data, see, e.g., refs. [10–14]). Its compatibility with particle physics models, where dissipation arises naturally from interactions in well-motivated quantum field theory models [15–17], further motivates its study. The recent advances in WI (see, for example [18] and references therein), underscore WI as a compelling bridge between early-universe cosmology and high-energy theory.

The model we study in this paper is an inflationary scenario involving an axion-like field with two cosine potentials, known as multi-natural inflation [19]. This setup is motivated by a broken global U(1) symmetry, in which a Peccei–Quinn field couples to two distinct sets of quarks, each charged under different non-Abelian gauge groups. We implement the multi-natural inflation model in the context of WI. In WI, the dissipation coefficient, denoted as Υ , quantifies the rate at which the inflaton field transfers energy to a thermal bath, sustaining radiation production during inflation. Its functional form, which usually can be a

function of the temperature T of the thermal radiation bath and the background inflaton field ϕ , depends on the underlying particle physics interactions and the regime of the inflaton's coupling to other fields (for a recent review, see also ref. [18]). Well-studied cases of the dissipation coefficient in WI include functional dependencies that can be linear or cubic in the temperature. These cases emerge for instance in cases where the inflaton is a pseudo-Goldstone boson [20–23]. Hence, these forms of dissipation coefficients studied here suit to the type of model we consider, since the multi-natural inflation model is an axion-like type of model.

By implementing the multi-natural inflation model in the context of WI, we show that in the case of the cubic dissipation coefficient, the scalar perturbations start to increase suddenly when a transition from a weak dissipation regime to a strong dissipation regime occurs at the later stage of the inflation. The tensor parts of perturbations cannot interact with scalar perturbations at linear order if the background spacetime is isotropic, though they can interact with each other nonlinearly [24, 25]. This indicates that scalar-induced tensor perturbations can be important only when the scalar perturbations take large values close to unity. We show that large scalar perturbations on small scales created during the warm multi-natural inflation with the cubic dissipation coefficient can give rise to abundant gravitational waves. Depending on the inflation energy scale, this gravitational wave spectrum can have a peak in the high-frequency regime around MHz, whose detection methods have been explored intensively [26, 28–33]. Moreover, its low-frequency tail may be detectable with future gravitational wave detectors such as DECIGO and ET. Therefore, the warm multi-natural inflation is testable with gravitational wave observations in principle.

The organization of the paper is as follows. In sec. 2, the WI scenario with a multi-natural axion potential is explained. In sec. 3, background equations of motion and perturbative equations are investigated in the warm multi-natural inflation with the two forms of dissipation coefficient considered in this paper. We derive approximate analytical expressions which helps to understand the behavior seen in the background dynamics and also the perturbations get affected in the model under study. In sec. 4, we numerically solve the equations of motion in the cases of the linear and cubic dissipation coefficients. The behavior of the dynamics that emerges in both cases are discussed. We also analyze the scalar power spectrum obtained in both cases. Here, we also investigate the dependence of the relevant background and perturbation quantities on the axion decay constant in the multi-natural inflaton potential. In sec. 5, we evaluate the scalar-induced gravitational waves on small scales. The focus is given in the case of the cubic dissipation coefficient, where the most notable results appear. Compatibility of our results with the bounds on the scalar power spectrum on small scales from light primordial black hole evaporation is also discussed. In sec. 6, we give our conclusions and final remarks. An appendix is also included to show and explain some key results that we have found.

2 warm multi-natural inflation

In the present implementation of WI, we work with an axion-like field ϕ that plays the role of the inflaton and which is coupled to a non-Abelian $SU(N_c)$ gauge field A_μ with the standard dimension five interaction,

$$\mathcal{L}_{\text{int}} = -\frac{g^2}{32\pi^2 f} \phi F_{\mu\nu}^c \tilde{F}^{c\mu\nu}, \quad (2.1)$$

where $c = 1, \dots, N_c^2 - 1$ is the group index, $F_{\mu\nu}^a = \partial_\mu A_\nu^a - \partial_\nu A_\mu^a + g\epsilon^{abc}A_\mu^b A_\nu^c$ is the gauge field tensor, $\tilde{F}^{c\mu\nu}$ is its dual,

$$\tilde{F}^{c\mu\nu} = \frac{\epsilon^{\mu\nu\rho\sigma}}{2a^3(t)} F_{\rho\sigma}^c, \quad (2.2)$$

$a(t)$ is the scale factor and $\epsilon^{\mu\nu\rho\sigma}$ is the usual Minkowski-like completely antisymmetrical tensor.

The interaction (2.1) is known to lead to a dissipation coefficient, which comes from nonperturbative sphaleron rate transitions at finite temperature in the gauge vacua, which is given by [22, 23]

$$\Upsilon_{\text{sph}}(T) = \kappa \frac{T^3}{f^2}, \quad (2.3)$$

where κ is given by

$$\kappa \simeq 1.2\pi \frac{g^4 (g^2 N_c)^3 (N_c^2 - 1)}{(64\pi^3)^2} \left[\ln \left(\frac{m_D}{\gamma} \right) + 3.041 \right], \quad (2.4)$$

where $m_D^2 = g^2 N_c T^2 / 3$ is the Debye mass squared of the Yang-Mills plasma and γ is given by the solution of [34]

$$\gamma = \frac{g^2 N_c T}{4\pi} \left[\ln \left(\frac{m_D}{\gamma} \right) + 3.041 \right]. \quad (2.5)$$

This gives for κ the result

$$\kappa = 0.3\alpha_g^5 N_c^3 (N_c^2 - 1) W \left(e^{3.041} \sqrt{\frac{4\pi}{3\alpha_g N_c}} \right), \quad (2.6)$$

where $\alpha_g = g^2 / (4\pi)$ is the fine structure Yang-Mills coupling and $W(x)$ is the Lambert function, given by the principal solution of $x = we^w$. If we assume, for example, $N_c = 3$ and $\alpha_g = 0.1$, this gives $\kappa \simeq 2.07 \times 10^{-3}$.

The result eq. (2.3) applies in the absence of fermions. By having fermions coupled to the gauge field, the Lagrangian density for the bath fields ($A_\mu^c, \psi, \bar{\psi}$) becomes

$$\mathcal{L}_{\text{bath}} = -\frac{1}{4} F_{\mu\nu}^c F^{c\mu\nu} + \bar{\psi} (i\mathcal{D} - m)\psi, \quad (2.7)$$

where $\mathcal{D} = \gamma^\mu D_\mu = \gamma^\mu (\partial_\mu + igA_\mu^c \mathcal{T}^c)$, with \mathcal{T}^c the generators of the non-Abelian gauge group. The presence of fermions tends to suppress the sphaleron dissipation in the case of chiral symmetry breaking ($m \neq 0$) and can even make it completely vanish, for massless fermions ($m = 0$). The effective dissipation in the presence of fermions become [35–37]

$$\Upsilon_{\text{eff}} = \Upsilon_{\text{sph}} \left(\frac{\Gamma_{\text{ch}}}{\Gamma_{\text{ch}} + 2\frac{f^2}{T^2} \Upsilon_{\text{sph}}} \right). \quad (2.8)$$

where Υ_{sph} is the pure gauge result eq. (2.3) and Γ_{ch} is given by

$$\Gamma_{\text{ch}} \sim N_c \alpha_g \frac{m^2}{T}, \quad (2.9)$$

where we are assuming that the chiral decay processes happen at a sufficiently large rate¹, $\Gamma_{\text{ch}} > H$, which can always be arranged by suitable choices of parameter, e.g. α_g and m . From eq. (2.8) we see that in the chiral limit $m \rightarrow 0$ the dissipation vanishes, for heavy fermions, $m \gg T, f$, we recover the result given by eq. (2.3), while for light fermions the dissipation becomes linearly dependent on the temperature,

$$\Upsilon_{\text{eff}} \simeq r N_c \alpha_g \frac{m^2}{2f^2} T. \quad (2.10)$$

The compatibility of WI in the context of QCD like values for the fermions (quarks) have been explicitly verified recently by the authors of ref. [37].

As explicitly verified in many recent works (see, for example refs. [23, 37, 39–42]), dissipation of the form of eq. (2.3) is able to lead to a consistent WI regime for a variety of inflaton potentials. The same is true for $\Upsilon \propto T$, as explicitly verified in many previous references [7, 11, 20, 43]. Yet, as far as standard axion-like cosine potentials are concerned, it is still a challenge to produce regimes of either cold or warm inflation for which the axion-decay constant is sub-Planckian, $f_a < M_{\text{Pl}}$ (see, e.g., refs. [42, 44] for some recent work in the context of axion WI). To overcome these issues with the standard axion-like cosine potential, in this paper we will work with a multi-natural axion like potential given by [19]

$$V(\phi) = V_0 \left[\cos\left(\frac{\phi}{f_a} + \theta\right) - \frac{\kappa}{n^2} \cos\left(n \frac{\phi}{f_a}\right) \right] + C, \quad (2.11)$$

where C is a constant, which is adjusted such that $V(\phi_{\text{min}}) = 0$ at its minimum. In the above potential f_a is the axion decay constant, while κ, θ and n are dimensionless constants. Here, we study this model in the context of WI with both cases of dissipation coefficients, given by eqs. (2.3) and (2.10). Following [45], we assume that $\kappa = 1$, n is an odd integer and $\theta \ll 1$. The motivation for using odd values stems from the fact that, in this case, the second derivatives of the potential at both its maximum and minimum are equal in magnitude but opposite in sign. When n is odd and increases, both the top and bottom of the potential become flatter at an equal rate. In multi-natural inflation, this offers several advantages. Firstly, it facilitates achieving inflation along the flatter top. Secondly, by appropriately setting the phase θ to be very small, the inflaton can be arranged to have a very small mass when it oscillates around the minimum. This allows the inflaton to be long-lived and potentially contribute to dark matter. Thus, by carefully tuning the potential's parameters, a sub-Planckian axion decay constant can be achieved while satisfying observational constraints for inflation (e.g. from Planck [46]), and an inflaton remnant could also serve as dark matter. While the first advantage (achieving inflation) could also be arranged for an even value of n ², the second (small inflaton mass and dark matter contribution) would not be possible.

3 Background dynamics and perturbation quantities in WI

The relevant background equations in WI are the evolution equations for the inflaton field and radiation energy density,

$$\ddot{\phi} + 3H\dot{\phi} + V_{,\phi} + \Upsilon\dot{\phi} = 0, \quad (3.1)$$

$$\dot{\rho}_r + 4H\rho_r = \Upsilon\dot{\phi}^2. \quad (3.2)$$

¹When $\Gamma_{\text{ch}} \ll H$, the effective dissipation eq. (2.8) changes [38, 39], but it still falls in an intermediate class of dissipation in between the two cases we consider here.

²Note that even values for n , e.g. $n = 2$, is also motivated from QCD axions [47].

For a thermalized radiation bath, we have that ρ_r is related to the temperature of the thermal bath as

$$\rho_r = C_r T^4, \quad (3.3)$$

where $C_r = g_* \pi^2/30$ and g_* denotes the radiation bath degrees of freedom. In the present work we assume that the radiation bath is constituted primarily by the gauge field fluctuations, which then gives $g_* = 2(N_c^2 - 1)$ for the case of the (massless) $SU(N_c)$ Yang-Mills fields³.

In WI, the slow-roll variables become [18]

$$\epsilon_H = -\frac{\dot{H}}{H^2} \simeq \frac{\epsilon_V}{1+Q}, \quad (3.4)$$

$$\eta = \frac{\eta_V}{1+Q}, \quad (3.5)$$

where $Q = \Upsilon/(3H)$ denotes the dissipation ratio in WI, while ϵ_V and η_V are the standard cold inflation slow-roll coefficients, defined, respectively, as

$$\epsilon_V = \frac{M_{\text{Pl}}^2}{2} \left(\frac{V_{,\phi}}{V} \right)^2, \quad (3.6)$$

$$\eta_V = M_{\text{Pl}}^2 \frac{V_{,\phi\phi}}{V}. \quad (3.7)$$

The general expression for the scalar of curvature perturbation spectrum in WI is [18]

$$P_{\mathcal{R}} \simeq \left(\frac{H_*^2}{2\pi\dot{\phi}_*} \right)^2 \left(1 + 2n_* + \frac{2\sqrt{3}\pi Q_*}{\sqrt{3+4\pi Q_*}} \frac{T_*}{H_*} \right) G(Q_*), \quad (3.8)$$

where n_* in the above expression denotes the possible statistical distribution for the inflaton due to the presence of the radiation bath, while the multiplicative function of the dissipation coefficient, $G(Q)$, in eq. (3.8) depends on the explicit form of the dissipation coefficient Υ , e.g. on how Υ depends on the temperature and inflaton amplitude⁴. The subindex $*$ in the quantities in eq. (3.8) means that they are evaluated at the Hubble crossing time, i.e., when $k = aH$.

The behavior of the power spectrum in WI is essentially dependent on the evolution of Q and T/H , which in turn depends on the form of the dissipation coefficient Υ and the inflaton potential. Parameterizing Υ for example like

$$\Upsilon(\phi, T) = C_{\Upsilon} T^c \phi^p M_{\text{Pl}}^{1-p-c}, \quad (3.9)$$

we have [41, 50]

$$\frac{d \ln Q}{dN} = C_Q^{-1} [(2c+4)\epsilon_V - 2c\eta_V - 4p\kappa_V], \quad (3.10)$$

$$\frac{d \ln(T/H)}{dN} = C_Q^{-1} \left[\frac{7-c+(5+c)Q}{1+Q} \epsilon_V - 2\eta_V - \frac{1-Q}{1+Q} p\kappa_V \right], \quad (3.11)$$

³When including also the inflaton fluctuations as thermalized, then $g_* = 2N_c^2 - 1$.

⁴Note that while $G(Q)$ depends mostly on the form of the dissipation coefficient, it is weakly dependent on the form of the inflaton potential [48, 49].

where $\kappa_V = M_{Pl}^2 V_\phi / (\phi V)$ and $C_Q = 4 - c + (4 + c)Q$ is a positive quantity, since Q is always positive and $-4 < c < 4$ is due to stability conditions in WI [51–53]. The eqs. (3.10) and (3.11) show that Q and T/H will grow during WI for $c > 0$ and for sufficiently concave potentials (where $\eta_V < 0$ during slow roll). Under these circumstances, the power spectrum $P_{\mathcal{R}}$ can increase during the WI dynamics. This effect has been explored recently in connection with the production of primordial black holes in WI [54–56] (for a slight different context, see also ref. [57] which also employs WI in the context of primordial black hole and gravitational wave generation). We will explore this ability of the power spectrum to grow during WI in connection to the model studied here.

In WI we need to enforce several constraining conditions, such as to avoid a strong back-reaction from the gauge field [58], enforce perturbativity ($\alpha_g < 1$) such that the calculation leading to eq. (2.3) remains valid, etc. These conditions typically lead to a hierarchy of energy scales [22, 23, 40, 58], $H < T < f < f_a$. In all of our examples, we observe that all these conditions remain satisfied.

In using eq. (3.8) for the scalar power spectrum in WI, we also need to check whether the inflaton will be thermalized with the thermal bath or not [59]. This determines, in particular, the presence or absence of the term n_* in eq. (3.8). For an interaction of the form of eq. (2.1) the dominant contribution for the thermalization of the inflaton (axion) with the gauge fields (thermal bath) comes from the scattering processes such as $\phi + A_\mu \rightleftharpoons A_\mu + A_\mu$, which occurs at a rate [60]⁵

$$\Gamma_{\phi+A_\mu \rightleftharpoons A_\mu+A_\mu} \sim \frac{\alpha_g^3 T^3}{32\pi f^2}. \quad (3.12)$$

Throughout our analysis we assume $n_* = 0$ in the eq. (3.8) for the power spectrum, which is equivalent to assume⁶ $\Gamma/H \ll 1$. In terms of the microscopic model leading to the present WI dynamics, e.g. through the axion-like interaction with the gauge fields, this can be achieved for sufficiently small gauge couplings and axion constant f . Finally, we also need to obtain the multiplicative function $G(Q)$ in eq. (3.8). Existing functions, which are obtained by fitting the numerical data for the perturbations in WI (see, e.g. refs. [41, 62, 63]) are valid in general for $n_* \sim n_{BE}$, i.e. assuming thermalization, $\Gamma > H$, and in which case n_* is approximated to a Bose-Einstein distribution [59]. Here, we generate the appropriate data for $G(Q)$ for the model and dissipation coefficients studied by explicitly evolving the perturbation equations in WI using the recently released `WI2easy` code for studying WI dynamics in general [49]. We refer the interested reader to ref. [49] for details. All our numerical results were obtained with the help of `WI2easy`. In fig. 1, we show the numerically generated results for $G(Q)$ for the two cases of dissipation coefficient considered here. Note that the results for $G(Q)$ are insensitive to the form of the potential, although it is strongly dependent on the form of the dissipation coefficient (see ref. [49]). The numerical data for $G(Q)$ is then interpolated using a spline method and used in the spectrum eq. (3.8) to derive the numerical results shown in the next section.

⁵The contributions from processes involving fermions of the thermal bath can also be included, but they contribute subdominantly to the rate when compared to the one due to the pure gauge field [60].

⁶Nevertheless, we have also studied the effect of including fully thermalized inflaton perturbations in our results, e.g., by assuming n_* takes the form of a Bose-Einstein distribution [61] and verified that all of our results do not change qualitatively.

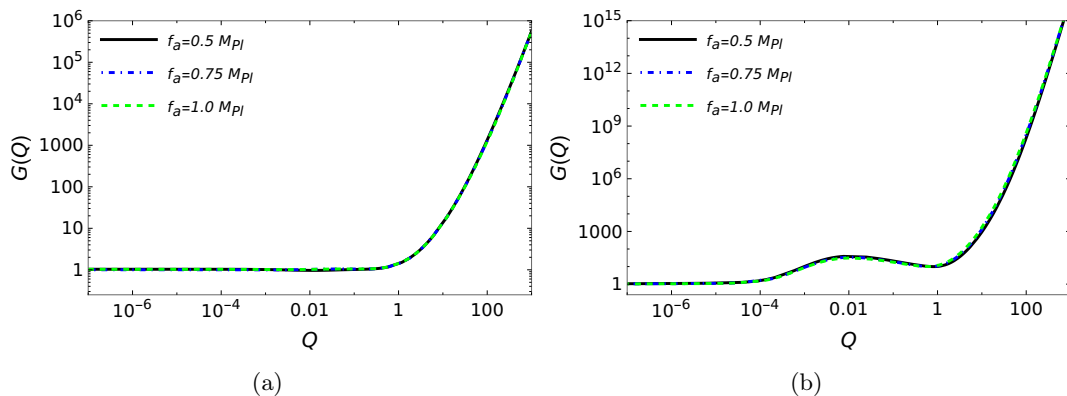


Figure 1. The $G(Q)$ function generated through `WI2easy` [49] for a dissipation coefficient eq. (3.9) for $c = 1, p = 0$ (panel a) and for $c = 3, p = 0$ (panel b) and obtained for three different values for the axion decay for the potential (2.11) (considering $n = 3, \kappa = 1$ and θ as given in tables 1 and 2 for each dissipation case, respectively). The nonthermal case $n_* = 0$ is considered.

4 Numerical Results

Keeping in mind the conditions and constraints discussed in the previous section, here we present our main numerical results when considering the potential eq. (2.11). As in ref. [45], we assume in the potential eq. (2.11) the parameters $\kappa = 1, n = 3$ and $\theta \ll 1$. The explicit value of θ is adjusted according to the dissipation ratio Q considered such that the spectral tilt n_s will fall close to the observational value $n_s \simeq 0.965$ from the Planck data⁷. We also observe that the dynamics is throughout in the WI regime, i.e., it satisfies $T/H > 1$, starting from the moment the observable quantities are computed (when the relevant CMB scales cross the Hubble radius), which happens around 60 e -folds before the end of inflation. Generically, this condition of having $T/H > 1$ requires that $Q \gtrsim 10^{-6}$ at the moment the relevant scales cross the Hubble radius.

As already mentioned, we consider the two cases of dissipation coefficients, with cubic and linear dependencies on the temperature, as motivated by eqs. (2.3) and (2.10), respectively. For a nonthermalized inflaton (see previous section) and for a thermal bath of pure gauge particles, the effective number of degrees of freedom is taken to be given by $g_* = 2(N_c^2 - 1)$ where we are considering $N_c = 3$.

To determine the point (N_*) where the relevant pivot scale crosses the Hubble radius during inflation, we use [65]

$$\frac{k_*}{a_0 H_0} = e^{-N_*} \left[\frac{43}{11g_s(T_{\text{end}})} \right]^{1/3} \frac{T_0}{T_{\text{end}}} \frac{H_*}{H_0} \frac{a_{\text{end}}}{a_{\text{reh}}}, \quad (4.1)$$

where $g_s(T_{\text{end}})$ is the entropy number of degrees of freedom at the end of inflation, taken here to be given by g_* for the models under consideration, $k_* = 0.05/\text{Mpc}$ is the typical pivot scale and which we also consider here, $a_0 = 1$ is the scale factor today, $H_0 = 67.66 \text{ km s}^{-1} \text{ Mpc}^{-1}$ (from the Planck Collaboration [66], TT,TE,EE-lowE+lensing+BAO 68% limits) and $T_0 = 2.725 \text{ K} \simeq 2.349 \times 10^{-13} \text{ GeV}$ is the present value of the CMB temperature. In the above

⁷We could also perform the analysis considering the most recent data results for n_s obtained from the Atacama Cosmology Telescope (ACT) [64], like done recently in ref. [14] in the context of WI. But this only affects our results very mildly.

equation, $a_{\text{end}}/a_{\text{reh}}$ gives the duration (in e -folds) lasting from the end of inflation until the beginning of the radiation dominated phase (determined by solving the background equations and tracking the point where the equation of state after WI becomes approximately 1/3). Finally, the normalization of the potential V_0 is determined by assuming that the scalar spectrum has the amplitude $\ln(10^{10}P_{\mathcal{R}}) \simeq 3.047$ (from the Planck Collaboration [66] TT,TE,EE-lowE+lensing+BAO 68% limits), at the pivot scale k_* .

4.1 Linear dissipation coefficient

Table 1. Parameters and results for r , n_s for the dissipation coefficient eq. (4.2), in the case of $n = 3$ and $\kappa = 1$ in the potential eq. (2.11).

f_a/M_{Pl}	θ	V_0/M_{Pl}^4	Q_*	ϕ_*/M_{Pl}	$\dot{\phi}_*/M_{\text{Pl}}^2$	$\rho_{r,*}/M_{\text{Pl}}^4$	C_Υ	n_s	r	N_*
0.5	2.5×10^{-4}	2.18×10^{-14}	9.96×10^{-7}	0.0216	4.55×10^{-11}	1.53×10^{-27}	2.60×10^{-6}	0.9670	1.24×10^{-6}	55.6
0.75	8.0×10^{-4}	1.08×10^{-13}	9.96×10^{-7}	0.0493	2.21×10^{-10}	3.62×10^{-26}	2.62×10^{-6}	0.9663	6.14×10^{-5}	56.1
1.0	1.9×10^{-3}	3.33×10^{-13}	9.96×10^{-7}	0.0878	6.94×10^{-10}	3.56×10^{-25}	2.60×10^{-6}	0.9663	1.90×10^{-5}	56.4

Let us first present the results for the case of a linear in the temperature dissipation coefficient,

$$\Upsilon = C_\Upsilon T, \quad (4.2)$$

where C_Υ is a dimensionless constant (for example, as given by the coefficient in eq. (2.10)). We analyze the cases where the axion decay constant f_a in the potential eq. (2.11) can assume the values $f_a = 0.5M_{\text{Pl}}$, $0.75M_{\text{Pl}}$ and $1M_{\text{Pl}}$. The relevant parameters and quantities evaluated in these three cases, when solving the background equations of WI (3.1) and (3.2) and from the power spectrum eq. (3.8) are summarized in Table 1.

In fig. 2 we show the evolution for the main background quantities, namely T/H , which confirms that we are in WI regime ($T/H > 1$) throughout the dynamics, the evolution of the dissipation ratio Q and also the evolution of the slow-roll coefficients in WI. In Fig 3 we show the power spectrum eq. (3.8), as a function of the scale, for the cases of the dissipation coefficient eq. (4.2) for the three cases of values f_a considered.

4.2 Cubic dissipation coefficient

Table 2. Parameters and results for r , n_s for the cubic in T dissipation coefficient $\Upsilon = C_\Upsilon T^3/M_{\text{Pl}}^2$, in the case of $n = 3$ and $\kappa = 1$ in the potential eq. (2.11).

f_a/M_{Pl}	θ	V_0/M_{Pl}^4	Q_*	ϕ_*/M_{Pl}	$\dot{\phi}_*/M_{\text{Pl}}^2$	$\rho_{r,*}/M_{\text{Pl}}^4$	C_Υ	n_s	r	N_*
0.5	1.5×10^{-3}	4.26×10^{-13}	9.11×10^{-7}	0.0229	9.14×10^{-10}	5.54×10^{-25}	7.43×10^6	0.9660	2.43×10^{-5}	55.5
0.75	3.8×10^{-3}	1.33×10^{-12}	9.04×10^{-7}	0.0527	2.81×10^{-9}	5.18×10^{-24}	2.43×10^6	0.9640	7.56×10^{-5}	55.7
1.0	7.2×10^{-3}	2.91×10^{-12}	8.97×10^{-7}	0.0965	6.14×10^{-9}	2.45×10^{-23}	1.12×10^6	0.9617	1.66×10^{-4}	56.0

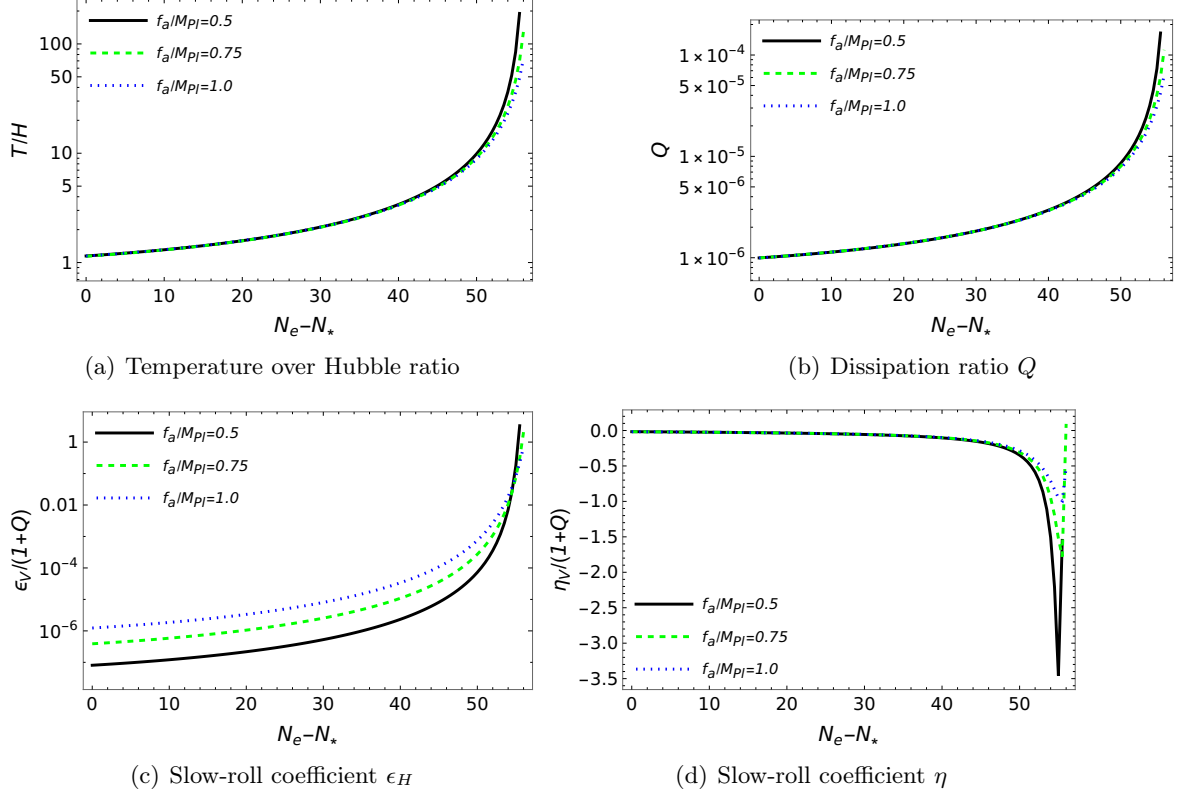


Figure 2. Main background quantities as a function of the number of e -folds for the case of the dissipation coefficient eq. (4.2).

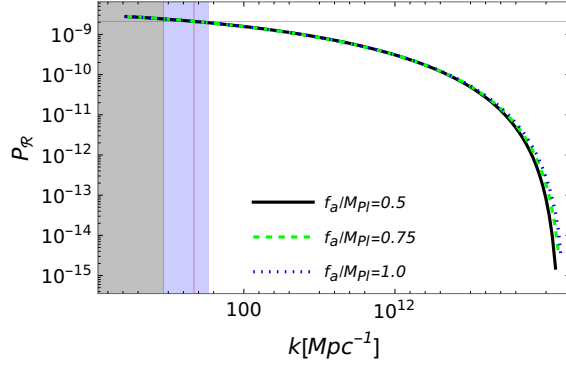


Figure 3. Power spectrum as a function of the scale for the case of the dissipation coefficient eq. (4.2). The left light blue region indicates the range of comoving modes values accessible through the current CMB data, $k_{\text{CMB}} \in [0.0005, 0.5] \text{Mpc}^{-1}$. The most to the left gray region indicates the range of comoving modes outside the horizon.

We now consider the results for the case of the dissipation coefficient of the form of eq. (2.3), i.e.,

$$\Upsilon = C_\Upsilon \frac{T^3}{M_{\text{Pl}}^2}, \quad (4.3)$$

where C_Υ is also a dimensionless constant (for example, as given by the coefficient in eq. (2.3)).

We once again analyze the same cases studied in the previous case of dissipation coefficient, by considering the axion decay constant f_a in the potential eq. (2.11) to have the values $f_a = 0.5M_{\text{Pl}}$, $0.75M_{\text{Pl}}$ and $1M_{\text{Pl}}$. The relevant parameters and quantities derived for this dissipation coefficient are now summarized in the Table 2.

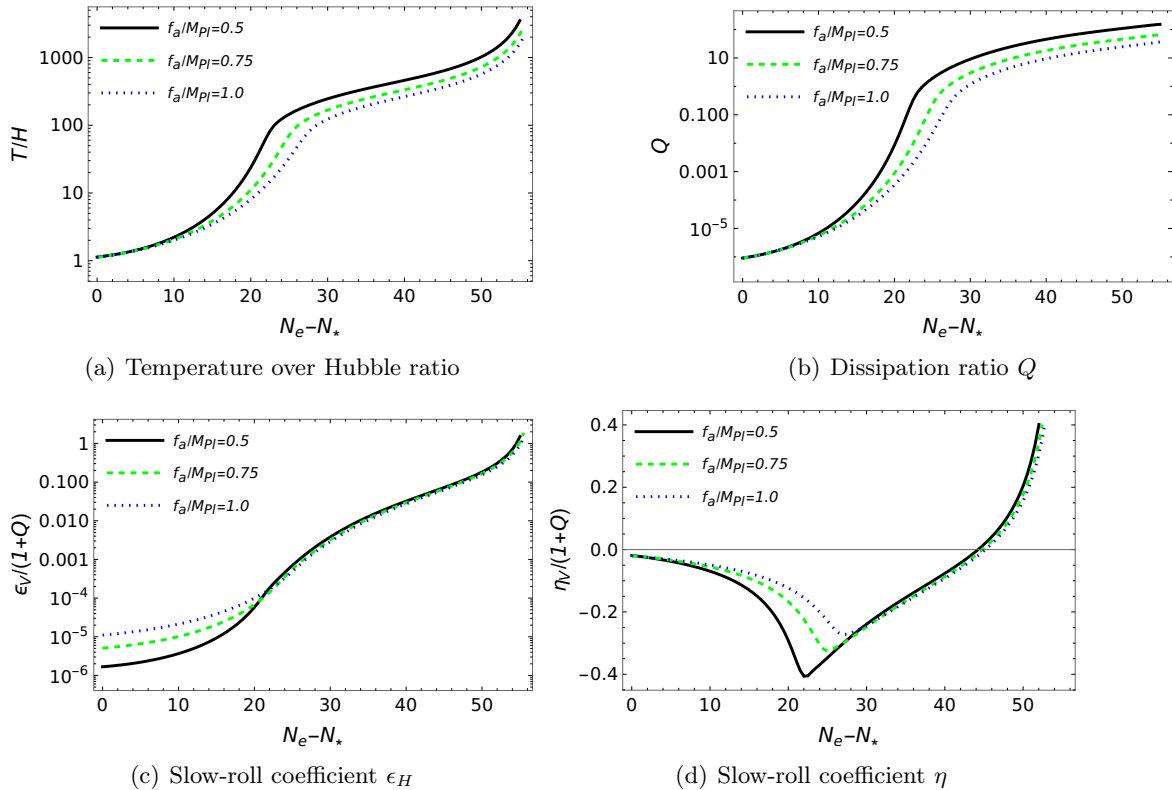


Figure 4. Main background quantities as a function of the number of e -folds for the case of the dissipation coefficient eq. (4.3).

In fig. 4 we show the evolution for the main background quantities, namely T/H , which also confirms that we are in WI regime ($T/H > 1$) throughout the dynamics, the evolution of the dissipation ratio Q and for the slow-roll coefficients in WI. In fig. 5 we show the power spectrum eq. (3.8) as a function of the scale that is obtained for the case of a cubic in the temperature dissipation coefficient in the multi-natural WI model.

4.3 Discussion of the results

From figs. 3 and 5, we see that while in the case of the dissipation coefficient which has a linear dependence on the temperature, the power spectrum always evolves such that to have less power at small scales, the situation inverts in the case of the dissipation coefficient with a cubic dependence on the temperature. In the cubic dissipation case, the power spectrum tends to grow significantly at the end of inflation. This is a consequence of both the form

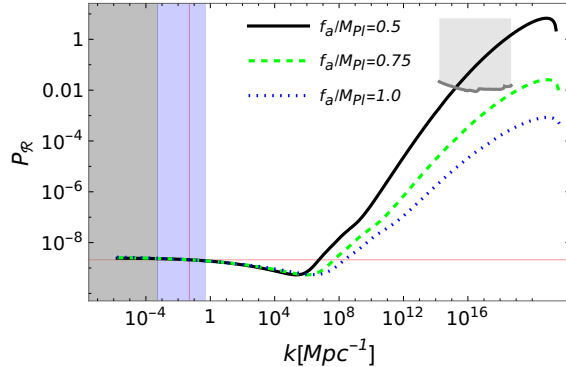


Figure 5. Power spectrum as a function of the scale for the case of the dissipation coefficient eq. (4.3). The top gray region is excluded due to nucleosynthesis bounds [67]. The left light blue region indicates the range of comoving modes values accessible through the current CMB data, $k_{\text{CMB}} \in [0.0005, 0.5] \text{Mpc}^{-1}$. The most to the left gray region indicates the range of comoving modes outside the horizon.

of the dissipation coefficient and the form of the potential, where inflation occurs mostly in the concave section of $V(\phi)$. We could anticipate this expectation based on the analytical expressions presented in the previous section (see the discussion in the paragraph below eq. (3.11)) and how they enter in the expression of the WI power spectrum eq. (3.8). As discussed, in the case of a dissipation coefficient with a cubic in the temperature dependence and for inflaton potentials that can have a concave part where inflation happens, like in the model under study, the power spectrum can exhibit rapid growth. In particular, linear cosmological perturbations can break down when the power spectrum goes above one. For the parameters assumed, for an axion decay constant $f_a \lesssim 0.75 M_{\text{Pl}}$, this can happen already for a very small dissipation ratio, $Q \gtrsim 10^{-6}$, and will become amplified for higher values of Q . Changing the potential parameters, in particular making θ smaller, to obtain a correct value for n_s we would need to increase Q initially, which would already put it at a value above the threshold leading to $P_{\mathcal{R}} > 1$ towards the end of inflation. From fig. 4, we see that the behavior of η_V , Q and T/H change drastically around the number of e -folds for which $Q \sim 1$. In fact, though η_V decreases before $Q \sim 1$, it suddenly starts to increase after the turning point. Indeed, we can trace the point where the power spectrum shown in fig. 5 stops losing power and transitions to a growing behavior exactly at this point. This feature has been observed in other WI models with different inflaton potentials [54–56].

Finally, we discuss the observational compatibility of the results obtained. There exist observational bounds on the fraction of primordial black holes (PBH) from their evaporation [67, 68]. The results in fig. 5 show that the power spectrum peaks at very small scales, close to the Big Bang Nucleosynthesis (BBN) scales. However, in general, it is not straightforward how to recast the bounds into those on the curvature perturbations. In fact, there are several uncertainties, such as the density-contrast threshold [67, 69], which can change the final result exponentially, when one calculates the fraction of PBH from a given power spectrum of curvature perturbations, and vice versa. Therefore, currently, we would not have a concrete way to evaluate the BBN bound on the scalar power spectrum through the primordial black hole evaporation. In fig. 5, we just compare an example of a BBN bound (top gray region in the plot) in the small scale power spectrum obtained in ref. [67] with our scalar power spectra, just as a benchmark. We can see that the case of $f_a = 0.5 M_{\text{Pl}}$ seems to be

incompatible with the BBN bound, while $f_a = 0.75M_{\text{Pl}}$ (marginally) and $f_a = 1.0M_{\text{Pl}}$ may be compatible with it.

For the linear dissipation case, the power spectrum remains well under control throughout the evolution up to the end of inflation. Typically, to obtain a consistent value for n_s also implies values for the dissipation ratio Q_* that are in the weak regime of WI. In this weak regime, $Q \ll 1$, there is no rapid growth of the power spectrum, in contrast to the cubic dissipation case.

In both cases of dissipation coefficients, in principle we could lower the axion decay constant f_a in the potential, but at the cost of further decreasing Q_* initially. Here in the multi-natural axion-type of potential eq. (2.11), we see a difficulty in achieving sub-Planckian axion decay constants and a consistent regime of WI, analogous to what also happens in vanilla single-axion cases [42, 44].

5 Induced gravitational waves

In the previous section, we saw that scalar fluctuations can grow on small scales for the case of the cubic dissipation coefficient, i.e. eq. (4.3). We also showed that there exist several parameter sets which give rise to the scalar power spectrum which may be compatible with the BBN bound. Interestingly, the magnitude of the power spectrum can still be large, of the order $\mathcal{O}(0.01)$ around the end of inflation. The tensor parts of perturbations do not interact with the scalar parts of perturbations at a linear level in an isotropic background universe. Thus, tensor and scalar fluctuations interact with each other only at the non-linear level [24, 25]. This is the reason why one can consider their evolution independently, since non-linear interactions are negligible in practice. However, when we have large scalar fluctuations, the non-linear interaction between tensor and scalar perturbations would not be negligible anymore. In fact, large scalar fluctuations can produce abundant gravitational waves [70]. In this section, we calculate the scalar-induced gravitational waves on small scales in the case of the cubic dissipation coefficient.

WI ends when the radiation energy density surpasses that of the inflaton, namely the radiation dominated era begins after the inflation ends⁸. Then, super-horizon modes of fluctuations created around the end of inflation experience re-entering in the radiation-dominated era. It is known that an approximated analytical expression of the power spectrum of gravitational waves produced by nonlinear scalar perturbations in the radiation dominated era is given by [71]

$$P_h(k) \simeq 4 \int_0^\infty dp \int_{|k-p|}^{k+p} dq \frac{p^2}{k^2 q^2} \left[1 - \left(\frac{k^2 + p^2 - q^2}{2kp} \right)^2 \right]^2 I^2(p, q, \eta) P_R(p) P_R(q), \quad (5.1)$$

where η is the conformal time and

$$I^2(p, q, \eta) \simeq \frac{1}{2} \left[\frac{3(p^2 + q^2 - 3k^2)}{4p^2 q^2 k \eta} \right]^2 \left\{ \left[4 - \left(\frac{p}{q} + \frac{q}{p} - \frac{3k^2}{pq} \right) \ln \left| \frac{3k^2 - (p+q)^2}{3k^2 - (p-q)^2} \right| \right]^2 + \pi^2 \left(\frac{p}{q} + \frac{q}{p} - \frac{3k^2}{pq} \right)^2 \theta(p+q - \sqrt{3}k) \right\}. \quad (5.2)$$

⁸In practice, it still can take around one to two e -folds of expansion after the end of WI before radiation energy density becomes dominant [50].

The power spectrum eq. (5.1) is related to the energy density parameter as

$$\Omega_{\text{GW}}(k, \eta) = \frac{k^2}{24a(\eta)^2 H(\eta)^2} P_h(k), \quad (5.3)$$

where $H(\eta)$ represents the Hubble parameter. The present spectra of Ω_{GW} induced by the scalar power spectra given in fig. 5 are shown in fig. 6, while assuming that the radiation dominant phase continues until the radiation-matter equality. One can see that the produced secondary gravitational waves can be tested with future gravitational wave detectors such as DECIGO, BBO, ET, and CE.

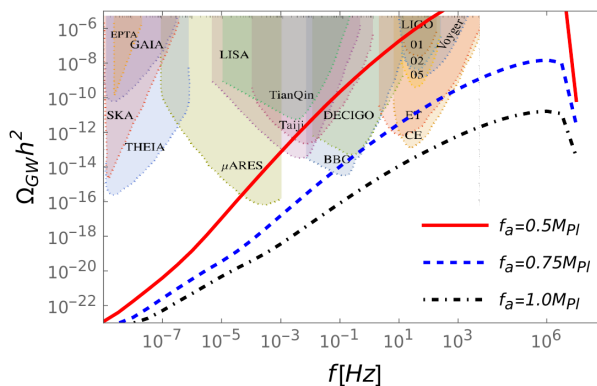


Figure 6. The spectrum of produced secondary gravitational waves as a function of frequency for the case of the dissipation coefficient eq. 4.3. The top shaded regions show the power-law integrated sensitivity for the current and future gravitational wave detectors (regions taken from fig.1 of ref. [72]).

It should be mentioned that an additional peak in a gravitational wave spectrum could appear at a lower frequency if a certain fraction of light PBH were produced [73–75] and a dominant PBH phase appeared. Although this possibility is interesting, we do not consider such a possibility. This is because there are several uncertainties, which can change the result exponentially, in the calculation of the fraction of primordial black holes from a given scalar power spectrum as discussed in the previous section.

6 Conclusion

In this paper, we studied multi-natural inflation in the context of WI. We studied the warm multi-natural inflation with dissipation coefficients that have either a linear or a cubic dependence on the temperature. These types of dissipation coefficients are well motivated in WI models where the inflaton is a pseudo-Goldstone scalar field, and they appear as limiting cases of dissipation from sphaleron decay from gauge and fermion interactions. It turned out that both cases could result in the spectral tilt and the tensor-to-scalar ratio, which are compatible with current observations. We also chose to closely follow the motivation for multi-natural inflation in producing both consistent inflationary observables and, eventually, a small mass for the inflaton at the end of inflation, such that the inflaton could also serve as dark matter. Therefore, we have considered only the case of an odd value for n in the potential eq. (2.11).

However, WI would also work similarly for even values of n leading to qualitatively similar results than the ones we have obtained. It is worth noting that in WI, as opposite to the case of CI, we found that a smaller axion decay constant leads to a larger enhancement of the power spectrum. This presents a challenge for the inflaton to also serve as dark matter in the scenarios proposed e.g. in ref. [45], as far as its implementation in WI is concerned.

As for the two cases of the dissipation coefficient that we have studied, we found that in the case of the cubic dissipation coefficient, in general, the curvature perturbation starts to increase suddenly when a transition from a weak to a strong dissipation regime occurs at the middle stages of the inflation dynamics. We have analyzed this behavior of the power spectrum for the model studied and its implications for both PBH formation and gravitational waves. We have calculated the scalar-induced gravitational waves from the large curvature perturbations on small scales. Interestingly, it was shown that gravitational waves may be detectable with future gravitational wave detectors such as DECIGO and ET. This indicates that the warm multi-natural inflation scenario is testable with gravitational wave observations in principle. Moreover, since the produced gravitational wave spectra have peaks around MHz, the development of new detection methods for high-frequency gravitational waves is encouraged [26–33].

It is worth to notice that while enhancements of the power spectrum in CI are typically achieved by tweaking the inflaton potential and adding features to it in some unnatural ways, in WI this is not necessary. For the type of potential we have considered, the enhancement of the power spectrum occurs naturally, with the dynamics already allowing the spectrum to change from red-tilted to blue-tilted. As for possible signatures that could distinguish this model from others, we would say that they would be the same signatures that would distinguish CI from WI. The most prominent one would be the differences in non-Gaussianities in the two scenarios (see ref. [6]). WI also does not satisfy the consistency relation between the tensor-to-scalar ratio and the tilt of the tensor spectrum, $r = -8n_t$, as observed in CI. Typically, we find that in WI, $r < 8|n_t|$ (see, e.g. refs. [7, 63]). Another distinctive feature of WI is also the possibility of the generation of matter isocurvature perturbations, due to the dissipative effects during inflation, that are fully anti-correlated with the dominant adiabatic curvature perturbations [76].

It should be mentioned that although we have not taken into account the non-Gaussianity of the curvature perturbations in the calculation of the induced gravitational waves, such an effect could change the tensor power spectrum slightly [77–79]. The non-Gaussianity of the curvature perturbations also can affect the fraction of created PBH, though its contribution is expected to be small [80]. Even apart from the effect of the non-Gaussianity, there still exist several uncertainties which can alter the result exponentially, like in the calculation of the fraction of PBH from a given scalar power spectrum, such as the density-contrast threshold [67, 69]. Therefore, for benchmark purposes, we just gave a comparison between an example of the BBN bound on the small scale power spectrum given in [67] and our scalar power spectra which have peaks right before the end of the inflation in the case of the cubic dissipation coefficient. Related to this point, we also assumed that there was no dominant PBH epoch after inflation, though it appears inevitably if certain amount of PBH are produced [74, 75]. Interestingly, if this is the case, not only the current gravitational wave spectrum is deformed, but also an additional peak could appear in the spectrum [73–75]. We hope these aspects will be revisited elsewhere in the future.

A Spectral tilt in the multi-natural WI model

In this appendix we derive approximate expressions for the spectral tilt n_s which helps to understand the behavior shown in figs. 3 and 5.

From eq. (3.8), the scalar spectral index n_s can be calculated at the horizon crossing (k_*) as

$$n_s - 1 = \left. \frac{d \ln P_{\mathcal{R}}}{d \ln k} \right|_{k \rightarrow k_*}, \quad (\text{A.1})$$

where, at Hubble radius crossing scale $k_* = aH$, we can write $d \ln k = (d \ln k / dN_e) dN_e$, $N_e = \ln a$ being the number of e -folds, then

$$\frac{d \ln k}{dN_e} \approx 1 - \epsilon_V / (1 + Q). \quad (\text{A.2})$$

From eq. (3.8), where we here consider $n_* = 0$ (see discussion following eq. (3.12)), together with (A.2), we then obtain for n_s the result

$$\begin{aligned} n_s - 1 = & \frac{-6\epsilon_V + 2\eta_V}{1 + Q - \epsilon_V} + \frac{d \ln Q}{dN} \frac{1 + Q}{1 + Q - \epsilon_V} \mathcal{A}(Q) \\ & + \frac{d \ln Q}{dN} \frac{-3 + (3 - 2\pi)Q + 2\pi Q^2 (3 + 2\sqrt{9 + 12\pi Q} \frac{T}{H})}{[3 + 2\pi Q (2 + \sqrt{9 + 12\pi Q} \frac{T}{H})] (1 + Q - \epsilon_V)} \\ & + \frac{d(\frac{T}{H})}{dN} \frac{2\pi Q(1 + Q)\sqrt{9 + 12\pi Q}}{[3 + 2\pi Q (2 + \sqrt{9 + 12\pi Q} \frac{T}{H})] (1 + Q - \epsilon_V)}, \end{aligned} \quad (\text{A.3})$$

with $d \ln Q / dN$ and $d(\frac{T}{H}) / dN$ given by eqs. (3.10) and (3.11), respectively, and the function $\mathcal{A}(Q)$ is defined by

$$\mathcal{A}(Q) = \frac{3 + 2\pi Q}{3 + 4\pi Q} + Q \frac{d \ln G(Q)}{dQ}. \quad (\text{A.4})$$

The expression (A.3) is a complicated expression in terms of the various parameters of the potential and also depends on the form of the dissipation coefficient. However, we can make some approximate expressions for the two cases of dissipation coefficients that we have considered, given by eqs. (4.2) and (4.3). Using eq. (A.3) together with eqs. (3.10) and (3.11), we find that n_s in the weak dissipative regime $Q \ll 1$ is given by

$$n_s \Big|_{Q \ll 1} - 1 \simeq -6\epsilon_V + 2\eta_V + \begin{cases} 10(\epsilon_V - \frac{\eta_V}{3})Q, & \text{for } \Upsilon \propto T, \\ (26\epsilon_V - 14\eta_V)Q, & \text{for } \Upsilon \propto T^3. \end{cases} \quad (\text{A.5})$$

In eq. (A.5) the first two terms on the right-hand side reproduce the standard CI result. The last term that depends on Q is the contribution of WI. One clearly sees that in both cases of dissipation in WI, the spectrum will be driven to become blue tilted when $\epsilon_V - \eta_V/3 > 0$ in the case of the dissipation coefficient (4.2), while that will tend to happen for $26\epsilon_V - 14\eta_V > 0$ in the case of the dissipation coefficient (4.3). We can also estimate the value of Q that the spectrum tends to transit from red to blue tilted. As a reference point, we can focus on the value for the inflaton where both background and spectrum tend to change most, which is

expected to happen around the inflection point of the potential⁹. From eq. (2.11) and for the parameters we are considering, the inflection point of the potential is

$$\phi_{\text{inf}} \simeq \frac{f_a}{2} \left(\pi - \frac{\theta}{2} \right). \quad (\text{A.6})$$

Hence, from eq. (A.5), we obtain that

$$n_s \Big|_{Q \ll 1, \phi = \phi_{\text{inf}}} - 1 \sim \begin{cases} \frac{9M_{\text{Pl}}^2}{8f_a^2} (2 + 3\theta) (-3 + 5Q), & \text{for } \Upsilon \propto T, \\ \frac{9M_{\text{Pl}}^2}{8f_a^2} (2 + 3\theta) (-3 + 13Q), & \text{for } \Upsilon \propto T^3. \end{cases} \quad (\text{A.7})$$

From eq. (A.7), we find that the spectrum will tend to change from red ($n_s < 1$) to blue ($n_s > 1$) for $Q \gtrsim 3/5$ in the case of a dissipation coefficient with linear temperature dependence, while for $\Upsilon \propto T^3$ the change occurs for $Q \gtrsim 3/13$. This explains the results for the scalar of curvature power spectrum obtained in the text for each case. From fig. 2(b) we see that for the parameters considered in the case of a dissipation coefficient with linear temperature dependence, Q is always much smaller than the red to blue transition value. Hence, the power spectrum for this case shown in fig. 3 decreases throughout the evolution. However, for the dissipation coefficient with a cubic temperature dependence, the turn-around point, as seen from fig. 4(b) already happens around 20 and 30 e-folds in the evolution, which also corresponds to the scales for which we see the behavior for the power spectrum changing in fig. 5. These results of the spectrum showing the change in behavior from red to blue also persist in the strong dissipative regime $Q > 1$. Although these results were obtained by choosing $n = 3$ in the potential, we have verified (although not shown here) that they also hold for other values of n . Furthermore, from eq. (A.7), we also explicitly see that the tilt of the spectrum (either in the red or blue directions) will be enhanced the more sub-Planckian ($f_a < M_{\text{Pl}}$) the axion decay constant becomes. This is fully consistent with the observed effect of changing the value of f_a also seen in figs. 3 and 5.

Acknowledgments

A.I. would like to thank Jan Tränkle for helpful discussions. A.I. was in part supported by JSPS KAKENHI Grant Number JP22K14034. R.O.R. acknowledges financial support by research grants from Conselho Nacional de Desenvolvimento Científico e Tecnológico (CNPq), Grant No. 307286/2021-5, and from Fundação Carlos Chagas Filho de Amparo à Pesquisa do Estado do Rio de Janeiro (FAPERJ), Grant No. E-26/201.150/2021.

References

- [1] A. Berera, Warm inflation, Phys. Rev. Lett. **75** (1995), 3218-3221
doi:10.1103/PhysRevLett.75.3218 [arXiv:astro-ph/9509049 [astro-ph]].
- [2] A. Berera, Thermal properties of an inflationary universe, Phys. Rev. D **54** (1996), 2519-2534
doi:10.1103/PhysRevD.54.2519 [arXiv:hep-th/9601134 [hep-th]].

⁹We note that for the dissipation coefficient $\Upsilon \propto T$ and for the parameters shown in table 1, inflation tends to end close to the inflection point of the potential. For $\Upsilon \propto T^3$, inflation tends to proceed beyond the inflection point and ends between this point and the minimum of the potential.

- [3] A. Berera, M. Gleiser and R. O. Ramos, Strong dissipative behavior in quantum field theory, *Phys. Rev. D* **58** (1998), 123508 doi:10.1103/PhysRevD.58.123508 [arXiv:hep-ph/9803394 [hep-ph]].
- [4] A. Berera, Interpolating the stage of exponential expansion in the early universe: A Possible alternative with no reheating, *Phys. Rev. D* **55** (1997), 3346-3357 doi:10.1103/PhysRevD.55.3346 [arXiv:hep-ph/9612239 [hep-ph]].
- [5] M. Bastero-Gil, A. Berera, I. G. Moss and R. O. Ramos, Cosmological fluctuations of a random field and radiation fluid, *JCAP* **05** (2014), 004 doi:10.1088/1475-7516/2014/05/004 [arXiv:1401.1149 [astro-ph.CO]].
- [6] M. Bastero-Gil, A. Berera, I. G. Moss and R. O. Ramos, Theory of non-Gaussianity in warm inflation, *JCAP* **12** (2014), 008 doi:10.1088/1475-7516/2014/12/008 [arXiv:1408.4391 [astro-ph.CO]].
- [7] M. Benetti and R. O. Ramos, Warm inflation dissipative effects: predictions and constraints from the Planck data, *Phys. Rev. D* **95** (2017) no.2, 023517 doi:10.1103/PhysRevD.95.023517 [arXiv:1610.08758 [astro-ph.CO]].
- [8] M. Bastero-Gil, S. Bhattacharya, K. Dutta and M. R. Gangopadhyay, Constraining Warm Inflation with CMB data, *JCAP* **02** (2018), 054 doi:10.1088/1475-7516/2018/02/054 [arXiv:1710.10008 [astro-ph.CO]].
- [9] R. Arya, A. Dasgupta, G. Goswami, J. Prasad and R. Rangarajan, Revisiting CMB constraints on warm inflation, *JCAP* **02** (2018), 043 doi:10.1088/1475-7516/2018/02/043 [arXiv:1710.11109 [astro-ph.CO]].
- [10] U. Kumar and S. Das, A generalized method of constraining Warm Inflation with CMB data, *JCAP* **10** (2024), 058 doi:10.1088/1475-7516/2024/10/058 [arXiv:2407.06032 [astro-ph.CO]].
- [11] F. B. M. d. Santos, R. de Souza and J. S. Alcaniz, A comparative analysis of dissipation coefficients in warm inflation, *JCAP* **10** (2024), 071 doi:10.1088/1475-7516/2024/10/071 [arXiv:2407.18891 [astro-ph.CO]].
- [12] F. B. M. d. Santos, G. Rodrigues, R. de Souza and J. S. Alcaniz, Stage IV CMB forecasts for warm inflation, *JCAP* **03** (2025), 062 doi:10.1088/1475-7516/2025/03/062 [arXiv:2412.02696 [astro-ph.CO]].
- [13] R. D'Agostino and M. Califano, New limits on warm inflation from pulsar timing arrays, *Phys. Dark Univ.* **48** (2025), 101910 doi:10.1016/j.dark.2025.101910 [arXiv:2406.01475 [astro-ph.CO]].
- [14] A. Berera, S. Brahma, Z. Qiu, R. O. Ramos and G. S. Rodrigues, The early universe is *ACT-ing warm*, [arXiv:2504.02655 [hep-th]].
- [15] A. Berera, I. G. Moss and R. O. Ramos, Warm Inflation and its Microphysical Basis, *Rept. Prog. Phys.* **72** (2009), 026901 doi:10.1088/0034-4885/72/2/026901 [arXiv:0808.1855 [hep-ph]].
- [16] M. Bastero-Gil, A. Berera and R. O. Ramos, Dissipation coefficients from scalar and fermion quantum field interactions, *JCAP* **09** (2011), 033 doi:10.1088/1475-7516/2011/09/033 [arXiv:1008.1929 [hep-ph]].
- [17] M. Bastero-Gil, A. Berera, R. O. Ramos and J. G. Rosa, General dissipation coefficient in low-temperature warm inflation, *JCAP* **01** (2013), 016 doi:10.1088/1475-7516/2013/01/016 [arXiv:1207.0445 [hep-ph]].
- [18] V. Kamali, M. Motaharfar and R. O. Ramos, Recent Developments in Warm Inflation, *Universe* **9** (2023) no.3, 124 doi:10.3390/universe9030124 [arXiv:2302.02827 [hep-ph]].
- [19] M. Czerny and F. Takahashi, Multi-Natural Inflation, *Phys. Lett. B* **733** (2014), 241-246 doi:10.1016/j.physletb.2014.04.039 [arXiv:1401.5212 [hep-ph]].

- [20] M. Bastero-Gil, A. Berera, R. O. Ramos and J. G. Rosa, Warm Little Inflaton, *Phys. Rev. Lett.* **117** (2016) no.15, 151301 doi:10.1103/PhysRevLett.117.151301 [arXiv:1604.08838 [hep-ph]].
- [21] M. Bastero-Gil, A. Berera, R. O. Ramos and J. G. Rosa, Towards a reliable effective field theory of inflation, *Phys. Lett. B* **813** (2021), 136055 doi:10.1016/j.physletb.2020.136055 [arXiv:1907.13410 [hep-ph]].
- [22] K. V. Berghaus, P. W. Graham and D. E. Kaplan, Minimal Warm Inflation, *JCAP* **03** (2020), 034 [erratum: *JCAP* **10** (2023), E02] doi:10.1088/1475-7516/2020/03/034 [arXiv:1910.07525 [hep-ph]].
- [23] M. Laine and S. Procacci, Minimal warm inflation with complete medium response, *JCAP* **06** (2021), 031 doi:10.1088/1475-7516/2021/06/031 [arXiv:2102.09913 [hep-ph]].
- [24] D. Baumann, P. J. Steinhardt, K. Takahashi and K. Ichiki, Gravitational Wave Spectrum Induced by Primordial Scalar Perturbations, *Phys. Rev. D* **76** (2007), 084019 doi:10.1103/PhysRevD.76.084019 [arXiv:hep-th/0703290 [hep-th]].
- [25] K. N. Ananda, C. Clarkson and D. Wands, The Cosmological gravitational wave background from primordial density perturbations, *Phys. Rev. D* **75** (2007), 123518 doi:10.1103/PhysRevD.75.123518 [arXiv:gr-qc/0612013 [gr-qc]].
- [26] N. Aggarwal, O. D. Aguiar, D. Blas, A. Bauswein, G. Cella, S. Clesse, A. M. Cruise, V. Domcke, S. Ellis and D. G. Figueroa, *et al.* Challenges and Opportunities of Gravitational Wave Searches above 10 kHz, [arXiv:2501.11723 [gr-qc]].
- [27] H. Matsuo and A. Ito, “Graviton-photon conversion in blazar jets as a probe of high-frequency gravitational waves,” [arXiv:2505.08457 [gr-qc]].
- [28] A. Ito, K. Kohri and K. Nakayama, Gravitational Wave Search through Electromagnetic Telescopes, *PTEP* **2024** (2024) no.2, 023E03 doi:10.1093/ptep/ptae004 [arXiv:2309.14765 [gr-qc]].
- [29] A. Ito and R. Kitano, Macroscopic quantum response to gravitational waves, *JCAP* **04** (2024), 068 doi:10.1088/1475-7516/2024/04/068 [arXiv:2309.02992 [gr-qc]].
- [30] A. Ito, K. Kohri and K. Nakayama, Probing high frequency gravitational waves with pulsars, *Phys. Rev. D* **109** (2024) no.6, 063026 doi:10.1103/PhysRevD.109.063026 [arXiv:2305.13984 [gr-qc]].
- [31] A. Ito and J. Soda, Exploring high-frequency gravitational waves with magnons, *Eur. Phys. J. C* **83** (2023) no.8, 766 doi:10.1140/epjc/s10052-023-11876-2 [arXiv:2212.04094 [gr-qc]].
- [32] A. Ito and J. Soda, A formalism for magnon gravitational wave detectors, *Eur. Phys. J. C* **80** (2020) no.6, 545 doi:10.1140/epjc/s10052-020-8092-6 [arXiv:2004.04646 [gr-qc]].
- [33] A. Ito, T. Ikeda, K. Miuchi and J. Soda, Probing GHz gravitational waves with graviton–magnon resonance, *Eur. Phys. J. C* **80** (2020) no.3, 179 doi:10.1140/epjc/s10052-020-7735-y [arXiv:1903.04843 [gr-qc]].
- [34] G. D. Moore and M. Tassler, The Sphaleron Rate in SU(N) Gauge Theory, *JHEP* **02** (2011), 105 doi:10.1007/JHEP02(2011)105 [arXiv:1011.1167 [hep-ph]].
- [35] K. V. Berghaus, P. W. Graham, D. E. Kaplan, G. D. Moore and S. Rajendran, Dark energy radiation, *Phys. Rev. D* **104** (2021) no.8, 083520 doi:10.1103/PhysRevD.104.083520 [arXiv:2012.10549 [hep-ph]].
- [36] M. Drewes and S. Zell, On sphaleron heating in the presence of fermions, *JCAP* **06** (2024), 038 doi:10.1088/1475-7516/2024/06/038 [arXiv:2312.13739 [hep-ph]].
- [37] K. V. Berghaus, M. Forslund and M. V. Guevarra, Warm inflation with a heavy QCD axion, *JCAP* **10** (2024), 103 doi:10.1088/1475-7516/2024/10/103 [arXiv:2402.13535 [hep-ph]].

- [38] K. V. Berghaus, M. Drewes and S. Zell, Warm Inflation with the Standard Model, [arXiv:2503.18829 [hep-ph]].
- [39] R. O. Ramos and G. S. Rodrigues, Viability of warm inflation with standard model interactions, *Phys. Rev. D* **111** (2025) no.12, 123527 doi:10.1103/wn1m-19gt [arXiv:2504.20943 [hep-ph]].
- [40] W. DeRocco, P. W. Graham and S. Kalia, Warming up cold inflation, *JCAP* **11** (2021), 011 doi:10.1088/1475-7516/2021/11/011 [arXiv:2107.07517 [hep-ph]].
- [41] S. Das and R. O. Ramos, Running and Running of the Running of the Scalar Spectral Index in Warm Inflation, *Universe* **9** (2023) no.2, 76 doi:10.3390/universe9020076 [arXiv:2212.13914 [astro-ph.CO]].
- [42] G. Montefalcone, V. Aragam, L. Visinelli and K. Freese, Observational constraints on warm natural inflation, *JCAP* **03** (2023), 002 doi:10.1088/1475-7516/2023/03/002 [arXiv:2212.04482 [gr-qc]].
- [43] G. Ballesteros, A. Perez Rodriguez and M. Pierre, Monomial warm inflation revisited, *JCAP* **03** (2024), 003 doi:10.1088/1475-7516/2024/03/003 [arXiv:2304.05978 [astro-ph.CO]].
- [44] S. Zell, No Warm Inflation From Sphaleron Heating With a Vanilla Axion, [arXiv:2408.07746 [hep-ph]].
- [45] R. Daido, F. Takahashi and W. Yin, The ALP miracle: unified inflaton and dark matter, *JCAP* **05** (2017), 044 doi:10.1088/1475-7516/2017/05/044 [arXiv:1702.03284 [hep-ph]].
- [46] Y. Akrami *et al.* [Planck], Planck 2018 results. X. Constraints on inflation, *Astron. Astrophys.* **641** (2020), A10 doi:10.1051/0004-6361/201833887 [arXiv:1807.06211 [astro-ph.CO]].
- [47] G. Grilli di Cortona, E. Hardy, J. Pardo Vega and G. Villadoro, The QCD axion, precisely, *JHEP* **01** (2016), 034 doi:10.1007/JHEP01(2016)034 [arXiv:1511.02867 [hep-ph]].
- [48] G. Montefalcone, V. Aragam, L. Visinelli and K. Freese, WarmSPy: a numerical study of cosmological perturbations in warm inflation, *JCAP* **01** (2024), 032 doi:10.1088/1475-7516/2024/01/032 [arXiv:2306.16190 [astro-ph.CO]].
- [49] G. S. Rodrigues and R. O. Ramos, WI2easy: warm inflation dynamics made easy, [arXiv:2504.17760 [astro-ph.CO]].
- [50] S. Das and R. O. Ramos, Graceful exit problem in warm inflation, *Phys. Rev. D* **103** (2021) no.12, 123520 doi:10.1103/PhysRevD.103.123520 [arXiv:2005.01122 [gr-qc]].
- [51] I. G. Moss and C. Xiong, On the consistency of warm inflation, *JCAP* **11** (2008), 023 doi:10.1088/1475-7516/2008/11/023 [arXiv:0808.0261 [astro-ph]].
- [52] M. Bastero-Gil, A. Berera, R. Cerezo, R. O. Ramos and G. S. Vicente, Stability analysis for the background equations for inflation with dissipation and in a viscous radiation bath, *JCAP* **11** (2012), 042 doi:10.1088/1475-7516/2012/11/042 [arXiv:1209.0712 [astro-ph.CO]].
- [53] S. del Campo, R. Herrera, D. Pavón and J. R. Villanueva, On the consistency of warm inflation in the presence of viscosity, *JCAP* **08** (2010), 002 doi:10.1088/1475-7516/2010/08/002 [arXiv:1007.0103 [astro-ph.CO]].
- [54] R. Arya, Formation of Primordial Black Holes from Warm Inflation, *JCAP* **09** (2020), 042 doi:10.1088/1475-7516/2020/09/042 [arXiv:1910.05238 [astro-ph.CO]].
- [55] M. Bastero-Gil and M. S. Díaz-Blanco, Gravity waves and primordial black holes in scalar warm little inflation, *JCAP* **12** (2021) no.12, 052 doi:10.1088/1475-7516/2021/12/052 [arXiv:2105.08045 [hep-ph]].
- [56] M. Correa, M. R. Gangopadhyay, N. Jaman and G. J. Mathews, Primordial black-hole dark matter via warm natural inflation, *Phys. Lett. B* **835** (2022), 137510 doi:10.1016/j.physletb.2022.137510 [arXiv:2207.10394 [gr-qc]].

- [57] P. B. Ferraz and J. G. Rosa, The inflation trilogy and primordial black holes, *JCAP* **03** (2025), 040 doi:10.1088/1475-7516/2025/03/040 [arXiv:2410.10996 [hep-ph]].
- [58] V. Kamali and R. O. Ramos, Thermal effects on warm chromoinflation, *JCAP* **01** (2025), 048 doi:10.1088/1475-7516/2025/01/048 [arXiv:2410.22624 [hep-ph]].
- [59] M. Bastero-Gil, A. Berera, R. O. Ramos and J. G. Rosa, Adiabatic out-of-equilibrium solutions to the Boltzmann equation in warm inflation, *JHEP* **02** (2018), 063 doi:10.1007/JHEP02(2018)063 [arXiv:1711.09023 [hep-ph]].
- [60] E. Masso, F. Rota and G. Zsembinski, On axion thermalization in the early universe, *Phys. Rev. D* **66** (2002), 023004 doi:10.1103/PhysRevD.66.023004 [arXiv:hep-ph/0203221 [hep-ph]].
- [61] R. O. Ramos and L. A. da Silva, Power spectrum for inflation models with quantum and thermal noises, *JCAP* **03** (2013), 032 doi:10.1088/1475-7516/2013/03/032 [arXiv:1302.3544 [astro-ph.CO]].
- [62] M. Bastero-Gil, A. Berera and R. O. Ramos, Shear viscous effects on the primordial power spectrum from warm inflation, *JCAP* **07** (2011), 030 doi:10.1088/1475-7516/2011/07/030 [arXiv:1106.0701 [astro-ph.CO]].
- [63] S. Bartrum, M. Bastero-Gil, A. Berera, R. Cerezo, R. O. Ramos and J. G. Rosa, The importance of being warm (during inflation), *Phys. Lett. B* **732** (2014), 116-121 doi:10.1016/j.physletb.2014.03.029 [arXiv:1307.5868 [hep-ph]].
- [64] E. Calabrese *et al.* [ACT], The Atacama Cosmology Telescope: DR6 Constraints on Extended Cosmological Models, [arXiv:2503.14454 [astro-ph.CO]].
- [65] S. Das and R. O. Ramos, Runaway potentials in warm inflation satisfying the swampland conjectures, *Phys. Rev. D* **102** (2020) no.10, 103522 doi:10.1103/PhysRevD.102.103522 [arXiv:2007.15268 [hep-th]].
- [66] N. Aghanim *et al.* [Planck], Planck 2018 results. VI. Cosmological parameters, *Astron. Astrophys.* **641** (2020), A6 [erratum: *Astron. Astrophys.* **652** (2021), C4] doi:10.1051/0004-6361/201833910 [arXiv:1807.06209 [astro-ph.CO]].
- [67] B. Carr, K. Kohri, Y. Sendouda and J. Yokoyama, Constraints on primordial black holes, *Rept. Prog. Phys.* **84** (2021) no.11, 116902 doi:10.1088/1361-6633/ac1e31 [arXiv:2002.12778 [astro-ph.CO]].
- [68] B. J. Carr, K. Kohri, Y. Sendouda and J. Yokoyama, New cosmological constraints on primordial black holes, *Phys. Rev. D* **81** (2010), 104019 doi:10.1103/PhysRevD.81.104019 [arXiv:0912.5297 [astro-ph.CO]].
- [69] B. Carr and F. Kuhnel, Primordial black holes as dark matter candidates, *SciPost Phys. Lect. Notes* **48** (2022), 1 doi:10.21468/SciPostPhysLectNotes.48 [arXiv:2110.02821 [astro-ph.CO]].
- [70] R. Saito and J. Yokoyama, Gravitational wave background as a probe of the primordial black hole abundance, *Phys. Rev. Lett.* **102** (2009), 161101 [erratum: *Phys. Rev. Lett.* **107** (2011), 069901] doi:10.1103/PhysRevLett.102.161101 [arXiv:0812.4339 [astro-ph]].
- [71] K. Kohri and T. Terada, Semianalytic calculation of gravitational wave spectrum nonlinearly induced from primordial curvature perturbations, *Phys. Rev. D* **97** (2018) no.12, 123532 doi:10.1103/PhysRevD.97.123532 [arXiv:1804.08577 [gr-qc]].
- [72] R. Roshan and G. White, Using gravitational waves to see the first second of the Universe, *Rev. Mod. Phys.* **97** (2025) no.1, 015001 doi:10.1103/RevModPhys.97.015001 [arXiv:2401.04388 [hep-ph]].
- [73] K. Inomata, M. Kawasaki, K. Mukaida, T. Terada and T. T. Yanagida, Gravitational Wave Production right after a Primordial Black Hole Evaporation, *Phys. Rev. D* **101** (2020) no.12, 123533 doi:10.1103/PhysRevD.101.123533 [arXiv:2003.10455 [astro-ph.CO]].

- [74] G. Domènech, C. Lin and M. Sasaki, Gravitational wave constraints on the primordial black hole dominated early universe, *JCAP* **04** (2021), 062 [erratum: *JCAP* **11** (2021), E01] doi:10.1088/1475-7516/2021/11/E01 [arXiv:2012.08151 [gr-qc]].
- [75] G. Domènech and J. Tränkle, From formation to evaporation: Induced gravitational wave probes of the primordial black hole reheating scenario, *Phys. Rev. D* **111** (2025) no.6, 063528 doi:10.1103/PhysRevD.111.063528 [arXiv:2409.12125 [gr-qc]].
- [76] M. Bastero-Gil, A. Berera, R. O. Ramos and J. G. Rosa, Observational implications of mattergenesis during inflation, *JCAP* **10** (2014), 053 doi:10.1088/1475-7516/2014/10/053 [arXiv:1404.4976 [astro-ph.CO]].
- [77] T. Nakama, J. Silk and M. Kamionkowski, Stochastic gravitational waves associated with the formation of primordial black holes, *Phys. Rev. D* **95** (2017) no.4, 043511 doi:10.1103/PhysRevD.95.043511 [arXiv:1612.06264 [astro-ph.CO]].
- [78] R. g. Cai, S. Pi and M. Sasaki, Gravitational Waves Induced by non-Gaussian Scalar Perturbations, *Phys. Rev. Lett.* **122** (2019) no.20, 201101 doi:10.1103/PhysRevLett.122.201101 [arXiv:1810.11000 [astro-ph.CO]].
- [79] C. Unal, Imprints of Primordial Non-Gaussianity on Gravitational Wave Spectrum, *Phys. Rev. D* **99** (2019) no.4, 041301 doi:10.1103/PhysRevD.99.041301 [arXiv:1811.09151 [astro-ph.CO]].
- [80] R. Saito, J. Yokoyama and R. Nagata, Single-field inflation, anomalous enhancement of superhorizon fluctuations, and non-Gaussianity in primordial black hole formation, *JCAP* **06** (2008), 024 doi:10.1088/1475-7516/2008/06/024 [arXiv:0804.3470 [astro-ph]].